A Theoretical Analysis Of The Transient Fluctuation Theorem For Accelerated Colloidal Systems In The Long-Time Limit

Yash Lokare[1]

1 Department of Physics, Indian Institute of Technology, Hauz Khas, New Delhi, India

The author confirms being the sole contributor of this work.
* ph1180857@iitd.ac.in

Abstract

A quantitative description of the second law of thermodynamics in small scale systems and over short time scales comes from various fluctuation theorems. The applicability of the transient fluctuation theorem in particular to small scale systems perturbed from an initial equilibrium steady-state distribution has been demonstrated both theoretically and experimentally in several works over the past few decades. In addition, some experimental works in the past have also made successful attempts to demonstrate the applicability of the fluctuation theorem to small scale systems evolving from a certain nonequilibrium steady-state distribution over relatively long time scales. To this end, this paper seeks to demonstrate the transient fluctuation theorem for a Brownian particle confined within a power-law trapping potential by following the trajectory of the particle that itself is translating linearly along one dimension with constant acceleration in a viscous fluid. Considered herein is an idealized version of this model, in that it is assumed that the force of the trapping potential is only felt by the translating Brownian particle confined within the trap, and that this Brownian particle moves relative to the fluid molecules that are held stationary. The results presented herein show that the transient fluctuation theorem applies not only to equilibrium steady-state distributions but also to nonequilibrium steady-state distributions of an ideal colloidal system in an *accelerated* frame of reference in the asymptotic (long-time) limit.

Introduction

The behavior of classical systems under the influence of external perturbations and microscopic forces has been a subject of long-standing interest amongst both theoreticians and experimentalists over the past several decades. At its heart, thermodynamics deals with a set of laws that govern the exchange of heat, work done and the entropy production and/or loss in a classical system [1] when in contact with another system or the environment. The characterisation of classical systems in thermodynamic equilibrium stems from equilibrium statistical mechanics in the microscopic domain which states that the probability of finding a classical system in a specific microstate (when in contact with a thermal reservoir) is simply given by the Boltzmann factor [2]. On the other hand, linear response theory allows one to characterise the dynamics of classical systems under very small deviations from equilibrium [1] through correlation functions derived under equilibrium conditions.

The quest of going beyond linear response theory and entering deep into the non-equilibrium regime to study how the exact thermodynamic relations applicable

under equilibrium conditions get modified when the thermodynamic properties of a classical system can no longer be described by equilibrium steady-state distribution functions has seen much development over the past few decades. Of particular interest has been the application of these general laws (derived under non-equilibrium conditions) to the realization of small scale systems such as nano-engines and protein motors. In essence, the idea is to scale down the sizes and/or dimensions of machines to accommodate a myriad of technological applications [3]. An important point to note is that if the work performed during the duty cycle of a machine is of the order of the thermal energy per degree of freedom, one could expect said machine to operate in 'reverse' over very short time scales [3]. By this, it is meant that the heat energy available in the surroundings could be extracted by the machine to perform useful work, which in turn would seemingly imply a violation of the second law of thermodynamics, in that entropy is being consumed rather than produced. One's main focus then shifts towards quantifying the probability of observing entropy consumption in small scale systems over short time scales. Loschmidt's paradox puts the second law of thermodynamics at odds with the time-reversal symmetry of almost all known fundamental physical processes operating at low-levels. It states that if there exists a motion of a system that leads to a reduction of entropy with time, then there definitely must exist another permissible state of the motion of said system, in which a steady increase in the entropy occurs with time. When put in the context of reversible microscopic equations of motion [3], this implies that in a classical system that respects time-reversal symmetry, for every phase-space classical trajectory, there must exist a time-reversed classical anti-trajectory (see [4]). The possibility of extrapolating such realizations to large scale systems would prove beneficial in circumventing the issues of low efficiency and increased losses.

A short note on stochastic thermodynamics: As understood in the context of the discussion and results that follow in this paper, stochastic thermodynamics applies to colloidal particles and other small scale systems such as biological motors, enzymes, and so forth. The following types of non-equilibrium situations can arise in such systems [1]: The system is prepared initially in a nonequilibrium state and is thereafter allowed to relax towards an equilibrium steady state. Also possible is the case when the system, initially in an equilibrium steady state, is acted upon by an external time-dependent driving force that pushes it towards a nonequilibrium steady state. Considering that in either case, the system maintains contact with an external thermal reservoir or a heat bath, its temperature, which is same as that of the thermal reservoir it is coupled to, remains well-defined throughout its temporal evolution. A consistent description of the thermodynamic properties of the system can then be constructed [1], by ensuring that an adequate time-scale separation be maintained between the adiabatically evolving degrees of freedom of the system and the rapidly-fluctuating degrees of freedom that are made up by the thermal reservoir. The thermodynamic states of the system are fully characterised and/or described by its adiabatically evolving degrees of freedom, in addition to certain fluctuations (that evolve on time scales much shorter than the slowly evolving degrees of freedom) that might be present in the system. The transition from one thermodynamic state to another constitutes a trajectory [1]. Busiello *et al.* much recently investigated the time-scale separation between adiabatically evolving degrees of freedom and rapidly evolving degrees of freedom in biology-inspired systems that incorporate a large number of multiple couplings between different allowed states (both, discrete and continuous), connected through different transition rates [5]. These are systems that typically operate in out-of-equilibrium conditions and in which, multiple couplings between different allowed states are active at a particular instant. Given the presence of multiple physical processes driving such systems at the same time, it becomes essential to treat these

systems at a coarse-grained level by employing a separation of time scales [5]. The authors propose a general framework to study stochastic systems involving multiple couplings between states, from which it becomes possible to analytically deduce the well-known laws and/or formulae of entropy production. This however is inherently dependent on the amount of information that is known about each process that drives any such system of interest out of equilibrium [5]. A separation of time scales allows the dynamics of the classical system under investigation to assume a Markovian nature.

Entropy production has long been considered as an essential feature and/or characteristic of systems operating in out-of-equilibrium conditions. The definition of 'entropy production' has however continued to remain vague in the context of stochastic systems, since there exist a number of classical systems that exhibit both, unidirectional and bidirectional transition characteristics between allowed states. To this end, Busiello *et al.* attempt to provide a consistent definition to entropy production in classical systems exhibiting such characteristics by employing a mapping scheme that preserves the average thermodynamic fluxes [6]. In addition, the authors analyze at length a certain class of stochastic systems composed of unidirectional links forming cycles as well as detailed-balance bidirectional links [6], demonstrating that these behave in a semi-deterministic manner. It is possible to numerically and experimentally simulate the distribution functions associated with the thermodynamic quantities of interest pertaining to a particular trajectory (for instance, the entropy loss and/or production, the heat exchanged with the thermal reservoir/environment, and so forth), as discussed and demonstrated in Refs. [3] and [7]– [11]. In general, one imposes the constraint that the system in question respect time-reversal symmetry to derive useful relations and theorems that quantify the distribution functions associated with the thermodynamic variables. As a consequence, 'entropy-consuming' trajectories that seem to violate the second law of thermodynamics manifest over typically short time scales. It however must be noted that this theoretical framework does not take into account the effects of fluctuations that might be present in the system [1]. If we interpret the second law of thermodynamics in a slightly different way, i.e., we instead talk about the mean entropy production and not merely the transient entropy consumption, the second law of thermodynamics in this sense is not violated. Furthermore, it can be shown that the probability of observing these entropy-consuming trajectories decays off exponentially over time, given which one must sample a very large number of transient trajectories of a classical thermodynamic system in order to observe these second law violations [12]. Specifically, if we assume the entropy production along a certain transient trajectory to be some quantity (hereby denoted as α), the theorem states that the ratio of the probability to observe an entropy-consuming trajectory to the probability of observing an entropy-producing trajectory (same magnitude, but with sign reversed) is given as (see Refs. [3], [12])

$$\frac{\mathrm{P}(\sigma_t = -\alpha)}{\mathrm{P}(\sigma_t = \alpha)} = \exp(-\alpha). \tag{1}$$

A large body of work in the past couple of decades has been dedicated to developing and extending this theorem further (see Refs. [13]– [24]).

In this paper, we demonstrate the applicability of the transient fluctuation theorem to classical systems by numerically following the trajectory of a Brownian particle confined within a harmonic trap and a quartic potential well which translate linearly in one dimension with a constant acceleration (whilst immersed in a viscous fluid). Further, we derive a general expression for the stochastic work done along transient classical trajectories for a Brownian particle confined within a power-law trapping potential, which is then tested and compared against numerical results. The numerical model presented in this paper closely resembles the experimental realization of the transient fluctuation theorem reported by Wang *et al.* [3].

Studies of fluctuation theorems involving colloidal particles in confining potentials

Numerous works over the recent years have experimentally and theoretically demonstrated the transient fluctuation theorem for colloidal particles confined in trapping potentials. Zon *et al.* for instance, used an overdamped Langevin equation for a Brownian particle confined in a harmonic trap to theoretically obtain the transient fluctuation theorem and the integrated stationary state fluctuation theorem for the case when an arbitrary motion of the focal point of the harmonic trap is considered [25]. Not long after, Carberry *et al.* directly demonstrated the transient fluctuation theorem for a confined Brownian particle in an experimental setting [26]. They did this by tracking in real-time the time-relaxation of a confined Brownian particle that underwent a step change in the depth of the optical trap held stationary over the course of the experiment. The experimental study of the thermodynamics of a Brownian particle confined in a time-dependent anharmonic trap was reported by Blickle *et al.* [27]. In this work, the authors demonstrate the validity of the first law of thermodynamics through the experimental estimation of the work done, heat exchanged and internal energy at the level of a single transient trajectory. Their results show that the probability distribution of the applied work along transient Brownian trajectories for this anharmonic trapping potential assumes a non-Gaussian profile, which bears excellent correspondence to numerical results. Also verified to a relatively good accuracy in their experimental realization of the transient FT are the Jarzynski relation and a detailed fluctuation theorem.

In light of some of the initial experimental realizations (i.e., in the early 2000s), Narayan *et al.* extended the analysis of the Jarzynski relation [28] and the transient fluctuation theorem in particle-dragging and polymer-stretching [29] experiments to provide a somewhat simpler proof for the transient fluctuation theorem for classical systems governed by Langevin dynamics [28] and generalize it to some extent for linearized versions of the Langevin equation. In 2005, Wang *et al.* demonstrated experimentally the steady-state fluctuation theorem from a single trajectory of a colloidal particle weakly confined in a moving optical trap [30]. Their setup closely resembled the one reported by Wang *et al.* [3] that sought to test the validity of the transient fluctuation theorem at colloidal length and time scales.

In recent years as well, there has been much development in the experimental realizations of fluctuation theorems for confined Brownian particles and/or nanoparticles. Pal *et al.* for instance, consider a numerical model of a Brownian particle confined in a harmonic trap whose focal point is continuously modulated in accordance with an Ornstein-Uhlenbeck process [31]. In this regard, the authors investigate the work fluctuations in this modulated trap within a certain time interval (the analysis is carried out in the steady state). Furthermore, they report on the calculations of the large deviation and the complete form of the probability distribution function of the stochastic work done by the Brownian particle in this modulated harmonic trap in the long-time limit. In 2014, Gieseler *et al.* investigated the case of a system that initially starts out in a nonequilibrium state but which gradually relaxes towards equilibrium [32]. Using a vacuum-trapped nanoparticle, they demonstrated the validity of a fluctuation theorem [32] for the entropy change that occurs during the relaxation process in an experimental setting. A comprehensive review of the potential use of optically-levitated nanoparticles in the study microscopic and stochastic thermodynamics appeared in 2018 [33]. The study of work fluctuations of active Brownian particles moving in viscoelastic mediums has also gained some traction in recent years. Narinder *et al.* for instance, experimentally investigate the work fluctuations of an active Brownian particle in a viscoelastic medium (the motion of the active Brownian particle is

self-propelled) [34]. Recent works have also shed light on the use of confined Brownian particles to study heat exchange between hydrodynamically coupled optical traps and investigate stationary and transient fluctuation theorems for effective heat fluxes between these traps [35], to investigate the out-of-equilibrium character of active matter systems [36], [37], and in the experimental realization of colloidal heat engines [38]- [40].

Materials and methods

Analytical description of the model

For a classical Newtonian system, it is customary to describe the system's state by an arbitrary point in phase space, which consists of the coordinates $\mathbf{q}$ and momenta $\mathbf{p}$ of all molecules and/or particles in the system. A point in phase space is typically represented as $\rho \equiv [\mathbf{q}, \mathbf{p}]$. The Newtonian equations of motion are time-reversible, which implies that for every classical trajectory that exists between points $\rho \equiv [\mathbf{q}_0, \mathbf{p}_0]$ and $\rho_{t^*} \equiv [\mathbf{q}_{t^*}, \mathbf{p}_{t^*}]$, there exists a time-reversed trajectory between points $\rho'_0 \equiv [\mathbf{q}_{t^*}, \text{-}\mathbf{p}_{t^*}]$ and $\rho'_{t^*} \equiv [\mathbf{q}_0, \text{-}\mathbf{p}_0]$. We now define a volume element for a set of classical trajectories at some arbitrary time instant t', as $\mathrm{dV}(\rho_{t'} \equiv [\mathbf{q}_{t'}, \mathbf{p}_{t'}])$, corresponding to which we will have a volume element for a set of time-reversed trajectories [3], which we denote as $\mathrm{dV}(\rho'_{t'} \equiv [\mathbf{q}_{t-t'}, \text{-}\mathbf{p}_{t-t'}])$. As seen previously [see Eq. 1], the reversibility of a system can be defined as the ratio of the probability of observing time-reversed trajectories to the probability of observing 'time-forward' trajectories. to this end, we evolve the system (and in turn, the transient classical trajectories) from an equilibrium steady-state distribution, for which the dynamics is well-known, i.e., the temporal evolution of the system begins at $t' = 0$. From Eq. 1, the dissipation function or equivalently, the stochastic work along a transient classical trajectory is given as

$$\sigma_t(\rho_0) = \ln\left[\frac{\mathrm{P}(\sigma_t > 0)}{\mathrm{P}(\sigma_t < 0)}\right]. \tag{2}$$

We consider a Brownian particle confined within a power-law trap which is translating linearly along one dimension (for the purpose of discussion, assume the motion to be along the x-axis) at constant acceleration. At a particular time instant t', we denote the position and momentum of the Brownian particle as $x_{t'}^*$ and $p_{t'}$, respectively. This power-law trap (and thus, the Brownian particle) moves in a viscous fluid and only the Brownian particle feels the effect of the confining potential (the neighboring fluid molecules do not feel any force and are held stationary relative to the moving Brownian particle). Also, we assume that the viscous fluid is maintained at a constant temperature, given which the application of the canonical ensemble to this system becomes possible. We denote this temperature as T. The Hamiltonian for this classical system can be expressed as the sum of the kinetic and potential energies of the system that arise as a result of intermolecular interactions and the confining potential. Also assumed in this model are very small displacements of the Brownian particle from its mean equilibrium position (i.e., the center of the trap) such that it never escapes the influence of the trapping potential. For the time-forward trajectories, the Hamiltonian assumes the form

$$H(\rho_0) = E_{\mathrm{K}}(p_0) + U_{\mathrm{int}}(x_0) + U_{\mathrm{trap}}(x_0^*), \tag{3}$$

where $E_{\mathrm{K}}(p_0)$ denotes the Brownian particle's kinetic energy and $U_{\mathrm{int}}(x_0)$ denotes the component of the potential energy that arises due to intermolecular interactions. Here, $U_{\mathrm{trap}}(x_0)$ denotes the potential energy of the confining potential. We note that $E_{\mathrm{K}}(p_0)$ and $U_{\mathrm{int}}(x_0)$ do not evolve over time, given which they remain *constant* throughout.

The confining potential assumes the form

$$U_{\text{trap}}(x) = \frac{k}{2n}(x_r)^{2n}, \tag{4}$$

where k is the trap stiffness constant and x_r denotes the position of the Brownian particle relative to the center of the trap at arbitrary time instances. Here, $n \in \mathbb{N}$. Note that we obtain bounded solutions only for even-exponent traps. For an odd-exponent trap, the Brownian particle will simply escape the influence of the confining potential. Since the trap is accelerating uniformly, the position of the trap center at an arbitrary time instant t^* can, from basic kinematics, be given as

$$x_{\text{trap}}(t^*) = \frac{1}{2}a_{\text{trap}}(t^*)^2, \tag{5}$$

where a_{trap} is the trap's acceleration. Note that the trap starts from rest at $t = 0$. Given Eq. 5, we have for x_r

$$x_r = x - \frac{1}{2}a_{\text{trap}}(t^*)^2. \tag{6}$$

Thus, from Eq. 4 and Eq. 6, the confining potential assumes the form

$$U_{\text{trap}}(x) = \frac{k}{2n}\left(x - \frac{1}{2}a_{\text{trap}}(t^*)^2\right)^{2n}. \tag{7}$$

In a similar manner, the Hamiltonian for the time-reversed trajectories assumes the form

$$H(\rho_0') = E_{\text{K}}(-p_t) + U_{\text{int}}(x_t) + U_{\text{trap}}(x_{t^*}), \tag{8}$$

where we have considered a time-reversal in the phase space coordinates. Also to be noted is that to respect time-reversal symmetry, the motion of the trap must begin at the position $\frac{1}{2}a_{\text{trap}}(t^*)^2$ for a time-reversed phase-space trajectory. Note that in a canonical ensemble, we have

$$P(dV(\rho_0)) \propto \exp\left(-\frac{H(\rho_0)}{k_B T}\right). \tag{9}$$

From Eq. 2 and Eq. 9, we have

$$\sigma_t(\rho) = \ln\left[\frac{\exp\left(-\frac{H(\rho_0)}{k_B T}\right)}{\exp\left(-\frac{H(\rho_0')}{k_B T}\right)}\right], \tag{10}$$

which on further simplification yields

$$\sigma_t(\rho) = \frac{1}{k_B T}\left(H(\rho_t) - H(\rho_0)\right), \tag{11}$$

where we have exploited the time-reversal symmetry that the transient trajectories obey. We can further simplify Eq. 11 by converting it into its integral form, as follows

$$\sigma_t(\rho) = \frac{1}{k_B T}\int_0^t \left(\frac{dH(\rho_{t^*})}{dt^*}\right)dt^*. \tag{12}$$

The term in the parentheses of the integrand in Eq. 12 can be expressed as the sum of the differentials of three energy terms appearing in the Hamiltonian of the system [see Eq. 3 and Eq. 8]. We consider these individually, as follows

$$\int_0^t \left(\frac{dU_{\text{trap}}(x_r)}{dt^*}\right)dt^* = \int_0^t k\left(x - \frac{1}{2}a_{\text{trap}}(t^*)^2\right)^{2n-1} \times \left(\frac{dx}{dt^*} - a_{\text{trap}}t^*\right)dt^*, \tag{13}$$

and a similar expression (in which the terms are accompanied by a negative sign) can be found for the kinetic energy. Following some simplification, we find that the stochastic work $\sigma_t(\rho)$ is given as

$$\sigma_t(\rho, n) = \frac{a_{\text{trap}}k}{k_B T} \int_0^t \left(x - \frac{1}{2} a_{\text{trap}}(t^*)^2 \right)^{2n-1} t^* dt^*, \tag{14}$$

where $x \equiv x(t)$ is the position of the Brownian particle within the trap at intermediate instances of time. Note that the acceleration a_{trap} remains constant throughout and we place the observer in the center-of-mass frame of the moving Brownian particle/trap.

Description of the numerical model

For the numerical tests, we allow the system to initially relax towards an equilibrium steady-state. The Brownian particle positions as a consequence, assume a Maxwellian-Boltzmann distribution before the trap is set in motion. The trap simulated has a stiffness constant of $k = 3.87 \times 10^{-7}$ N/m. We consider the viscosity of the fluid to be $\eta = 2.5$ Poise and the radius of the Brownian particle to be $R = 9.23$ μm. In the case of the harmonic trap, the temperature of the fluid (the thermal reservoir) is maintained at 400 K, whereas for the case of the quartic potential well, we maintain a constant temperature of $T = 433$ K throughout the motion. The friction constant for the fluid medium is, by Stoke's law, given as $\gamma = 6\pi\eta R$. Note that the position of the particle within the trap at intermediate time instances is computed using the Langevin equation, given as

$$m \frac{d^2 x}{dt^2} = -\frac{\partial U_{\text{trap}}(x)}{\partial x} - \gamma \frac{dx}{dt} + \xi(t), \tag{15}$$

where m is the mass of the Brownian particle and $\xi(t)$ is a delta-correlated Gaussian white noise term that satisfies $\langle \xi(t)\xi(t') \rangle = 2\gamma k_B T \delta(t - t')$. In the numerical model, we implement $\xi(t)$ using a Gaussian random number generator. Note that here, we consider an overdamped Langevin equation, in which case γ is large enough that the inertia term, i.e., the LHS of Eq. 15 drops out. The trap is set in motion for 20 seconds, starting from $t = 0$, from which we sample out transient classical trajectories of different lengths (i.e., over different time scales). The sub-trajectories of a transient trajectory in each case are spaced 4 ms apart (i.e., the time step implemented in the numerical model). The trap is accelerated uniformly at $a_{\text{trap}} = 4 \times 10^{-7}$ m/s^2. The initial position of the Brownian particle relative to the bottom of the sample cell is 0.85 μm, whereas the initial distance of the center of the trap relative to the bottom of the sample cell is 0.35 μm. We use Eq. 14 to model the stochastic work done by the Brownian particle along transient classical trajectories.

Numerical results

Of interest to us is the determination of a closed-form expression for the temporal dependence of the probability density function of σ_t. A detailed analysis of the same appears in Ref [10]. Presented in this section is an outline of the derivation for the case of a harmonic trap (a similar (albeit more complicated) calculation is possible for the case of a quartic potential well (x^4 potential)).

We set $m = 1$ for simplicity. Note that in Eq. 14, we replace the terms appearing inside the integral by F_{trap} for the sake of notational convenience. Eq. 14 then reads

$$\sigma_t = \frac{a_{\text{trap}}}{k_B T} \int_0^t F_{\text{trap}}(t^*) dt^*. \tag{16}$$

It is essential to note that although the derivation of Eq. 14 follows form a deterministic dynamics treatment, the derivation of a closed form expression for $P(\sigma_t)$ will follow from a stochastic dynamics treatment (due to the presence of the stochastic force term $\xi(t)$). Note that at any time t, the condition $F_{\text{drag}} + F_{\text{trap}} + F_{\text{stochastic}} = 0$ is satisfied, given which the force due to the confining potential in the overdamped limit assumes the form $F_{\text{trap}} = \gamma dx/dt - \xi(t)$ [see Eq. 15]. Plugging this definition into Eq. 16, we get

$$\sigma_t = \frac{a_{\text{trap}}\gamma}{k_B T}\big(x(t) - x_0 - \Omega(t)\big), \tag{17}$$

where $x(t)$ denotes the position of the Brownian particle within the trap and $\Omega(t)$ is given as $\Omega(t) = \frac{1}{\gamma}\int_0^t \xi(t^*)dt^*$. Here, x_0 denotes the equilibrium position of the Brownian particle within the trap before it is set in motion (i.e., before the initial transient). We see that the contribution proportional to the displacement of the Brownian particle within the trap, i.e., $\propto [x(t) - x_0]$ arises from the viscous drag force that the fluid exerts on the Brownian particle, whereas the contribution $\Omega(t)$ arises as a consequence of the presence of the stochastic force term $\xi(t)$ [10]. The analysis can be made simpler by making a coordinate transformation, i.e., a transformation to a reference frame co-moving with the trap. In this case, we have $r(t) = x_0 + 1/2a_{\text{trap}}t^2 - a_{\text{trap}}\gamma^2/k^2$ and $r_0 = x_0 - a_{\text{trap}}\gamma^2/k^2$. Eq. 17 in this frame can then be recast as

$$\sigma_t = \frac{a_{\text{trap}}\gamma}{k_B T}\left(x(t) + \frac{1}{2}a_{\text{trap}}t^2 - x_0 - \Omega(t)\right). \tag{18}$$

Note that $\tau \equiv \gamma/k$ is the characteristic time scale of the system's motion. Since the Brownian particle was allowed to thermalize initially, we know that x_0 assumes a Maxwellian-Boltzmann distribution. The general form of the solution to the stochastic differential equation for $x(t)$ is given as

$$x(t) = x_0 \exp\left(-\frac{t}{\tau}\right) + \int_0^t \frac{\xi(t^*)}{\gamma}\exp\left(-\frac{(t - t^*)}{\tau}\right)dt^*. \tag{19}$$

Given Eq. 18, we see that to compute the probability distribution function of σ_t, it is essential that we obtain a closed-form expression for $P\big(x(t) - \Omega(t)\big)$. From Eq. 19, we see that $x(t) - \Omega(t)$ (which we denote as $\psi(t)$) assumes the form

$$\psi(t) = x_0 \exp\left(-\frac{t}{\tau}\right) + \int_0^t \frac{\xi(t^*)}{\gamma}\left[\exp\left(-\frac{(t - t^*)}{\tau}\right) - 1\right]dt^*. \tag{20}$$

We see that Eq. 20 consists of a sum of terms, all of which are Gaussian distributed (since x_0 assumes a Maxwellian-Boltzmann distribution, and $\xi(t)$ is a delta-correlated Gaussian white noise term). Thus, we can conclude that the distribution of $\psi(t)$ will also be a Gaussian distribution, the general form of which can be expressed as [10]

$$P(\psi(t)) = \frac{1}{\sqrt{2\pi\theta(t)}}\exp\left(-\left(\frac{\psi(t) - \mu(t)}{\sqrt{2\theta(t)}}\right)^2\right), \tag{21}$$

where $\theta(t)$ denotes the distribution's time-dependent standard deviation and $\mu(t)$ denotes the mean. Note that $P(\psi(t)) \equiv P(\psi(t), x_0, t)$ is the probability of finding $\psi(t)$ at $x = x_0$ and at time t [10]. Since the distribution of $\psi(t)$ is expected to be Gaussian [see Eq. 21], we can directly compute $\mu(t)$ by taking the ensemble average of Eq. 20. Noting that the ensemble average of the stochastic force term $\xi(t)$ vanishes, i.e., $\langle\xi(t)\rangle = 0$, we see that $\mu(t) = x_0 \exp(-t/\tau)$. Further, we compute $\theta(t)$ as [10]

$$\theta(t) = \langle\big(\psi(t) - \mu(t)\big)^2\rangle = \int_0^t dt_1 \int_0^t \frac{dt_2}{\gamma}\left[\exp\left(-\frac{(t - t_1)}{\tau}\right) - 1\right] \times \left[\exp\left(-\frac{(t - t_2)}{\tau}\right) - 1\right]$$
$$\langle\xi(t_1)\xi(t_2)\rangle. \tag{22}$$

Note that $\xi(t)$ is a delta-correlated noise term, i.e., $\langle \xi(t_1)\xi(t_2) \rangle = 2\gamma k_B T \delta(t_1 - t_2)$. Plugging this definition into Eq. 22 and integrating, we obtain for $\theta(t)$

$$\theta(t) = \frac{k_B T}{\gamma}\left(2t + 4\tau \exp\left(-\frac{t}{\tau}\right) - \tau \exp\left(-\frac{2t}{\tau}\right) - 3\tau\right). \tag{23}$$

The distribution of x_0 assumes the form [10]

$$P(x_0) = \sqrt{\frac{k}{2\pi k_B T}} \exp\left(-\frac{k}{2k_B T}\left(x_0 - \frac{a_{\text{trap}}\gamma^2}{k^2}\right)^2\right). \tag{24}$$

From Eqs. 21 through 24, one can compute the full distribution of $\psi(t)$. From Eq. 18, we obtain $\psi(t) = k_B T \sigma_t / a_{\text{trap}}\gamma + x_0 - 1/2a_{\text{trap}}t^2$, where we use the fact that $\psi(t) = x(t) - \Omega(t)$. Integrating over x_0 yields [10]

$$P(\sigma_t) = \frac{k_B T}{a_{\text{trap}}\gamma} \int_{-\infty}^{\infty} dx_0 P\left(k_B T \sigma_t / a_{\text{trap}}\gamma + x_0 - 1/2a_{\text{trap}}t^2, x_0, t\right) P(x_0). \tag{25}$$

As in [10], we introduce the following time-dependent function

$$\phi(t) = \Delta^2\left(\frac{t}{\tau} - \left(1 - \exp\left(-\frac{t}{\tau}\right)\right)\right), \tag{26}$$

where Δ is a dimensionless factor that is defined as the ratio of the motion's lag distance (i.e., $\equiv a_{\text{trap}}\gamma^2/k^2$) to the characteristic length scale of the system (or more precisely, the motion), given as $\sqrt{k_B T/k}$. Essentially, Δ is a convenient measure of the opposing forces that act on the Brownian particle localized within the trap [10]. Solving Eq. 25 then yields the following for the probability distribution of σ_t

$$P(\sigma_t) = \frac{1}{\sqrt{\pi\phi(t)}} \exp\left(-\frac{1}{4\phi(t)}\left(\sigma_t - \phi(t)\right)^2\right), \tag{27}$$

where we note that the time-dependent mean of the distribution $\mu(t) \equiv \phi(t)$. We thus see that the probability distribution of σ_t is a Gaussian whose peak moves with time. The implications of this as well as its physical interpretation is discussed in the next section. Note that this derivation is only applicable for a harmonic trapping potential. This is because from Eq. 15, we see that unlike the harmonic trapping case, a term proportional to x^3 would appear (i.e., the differential term on the RHS of Eq. 15) for the quartic trapping potential case, for which the derivation presented above does not hold.

Harmonic trap

Consider first the case of the harmonic trap, for which we set $n = 1$ in Eq. 14 to numerically compute and model the stochastic work done by the Brownian particle along transient classical trajectories. For this, we consider the entropy production and/or consumption along trajectories of different lengths (i.e., sampled over different time scales). The probability distributions are computed numerically at different time instances.

By employing the maximum likelihood estimation method, we fit a Gaussian to each of the histogram distributions depicted in Fig. 1, the results of which are shown in Fig. 2.

As predicted analytically, we see that the peaks or equivalently, the mean of the distributions moves towards positive σ_t with time. Moreover, we note that the variance of the distributions or equivalently, the spread in the probability distributions of σ_t increases with time, which given the time-dependent nature of $\phi(t)$, as it appears in
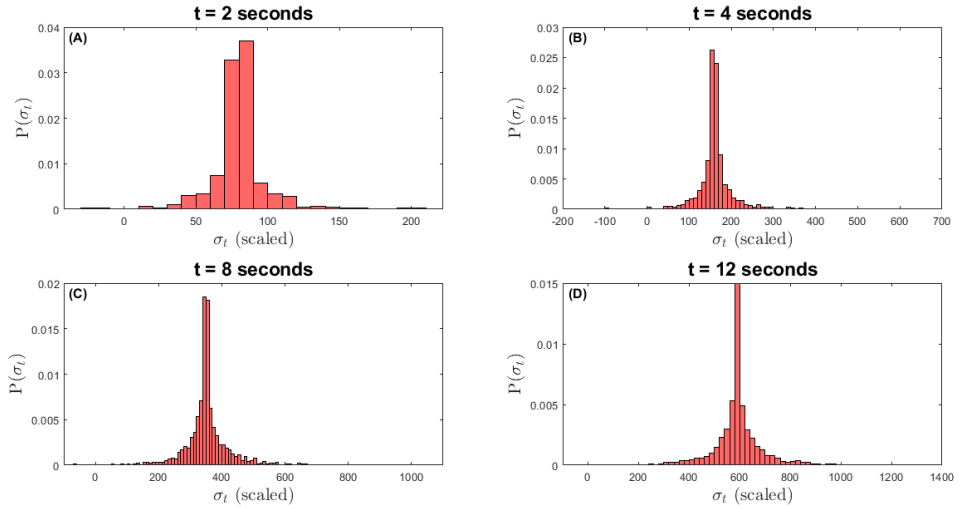
Fig 1. (Color outline) Probability distributions of the stochastic work done by a Brownian particle confined within a uniformly accelerating harmonic trap.
A) Probability distribution of σ_t (stochastic work) computed at $t = 2$ seconds. **B**) Probability distribution of σ_t (stochastic work) computed at $t = 4$ seconds. **C**) Probability distribution of σ_t (stochastic work) computed at $t = 8$ seconds. **D**) Probability distribution of σ_t (stochastic work) computed at $t = 12$ seconds. Note that in accord with Eq. 27, the peaks of the distributions move towards positive σ_t with the passage of time.
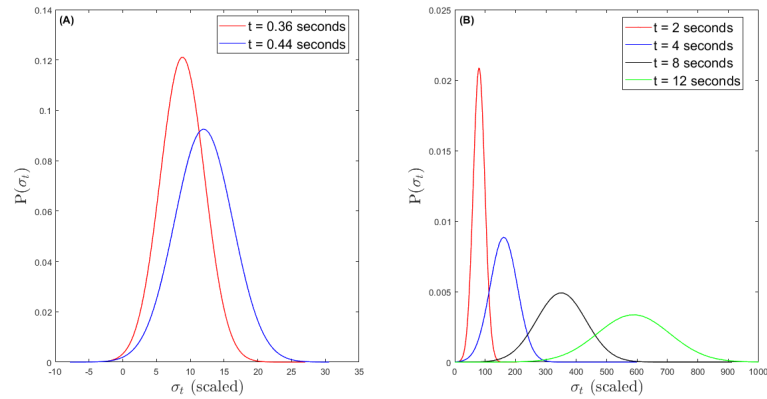
Fig 2. (Color outline) Gaussian fits to the probability distributions of σ_t at different time instances.
A) Gaussian fits to the probability distributions of σ_t computed at $t = 0.36$ seconds (solid red line) and $t = 0.44$ seconds (solid blue line), respectively. **B**) Gaussian fits to the probability distributions of σ_t computed at $t = 2$ seconds (solid red line), $t = 4$ seconds (solid blue line), $t = 8$ seconds (solid black line) and $t = 12$ seconds (solid green line). Note that in accord with Eq. 27, the peaks of the distributions move towards positive σ_t with the passage of time.

Eq. 27, is an expected outcome. It must be noted that Fig 2A has also been obtained via a Gaussian fit to the probability distributions of σ_t computed at $t = 0.36$ seconds

and $t = 0.44$ seconds, respectively. An important point to consider is the probability of observing entropy-consuming trajectories over certain time scales. To be noted from Fig. 2 is the fact that for times ≥ 2 seconds, the probability of observing entropy-consuming trajectories reduces to zero. On the other hand, we see that for times below 0.5 seconds (more specifically, 0.36 seconds and 0.44 seconds, as depicted in Fig. 2), there exists a finite probability of observing phase-space classical anti-trajectories (with the tail of the distributions extending towards negative values of σ_t). A further verification of this observation is presented in Fig. 3, where we note the rapid decrease in the probability of observing phase-space classical anti-trajectories. We see that the probability $P(\sigma_t < 0)$ is finite for times below 0.5 seconds, which beyond 0.5 seconds reduces to zero. This is also in accord with Eq. 1, which predicts the exponential decrease of $P(\sigma_t < 0)$ with time, until a point after which no entropy-consuming trajectories are observed.
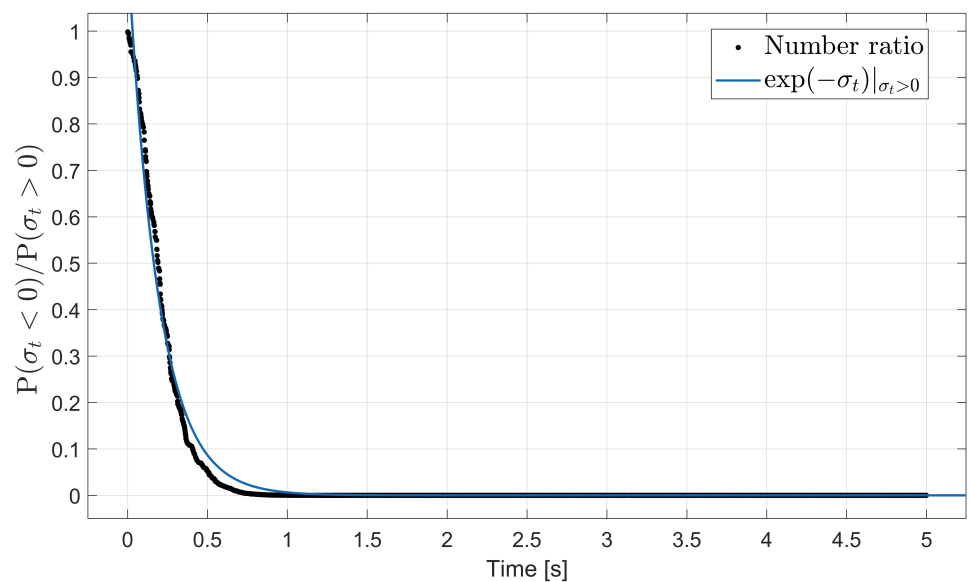
Fig 3. (Color outline) Plot for the number ratio of entropy-consuming to entropy-producing classical trajectories vs. time.
Plot for the number ratio of entropy-consuming to entropy-producing classical trajectories (i.e., $P(\sigma_t < 0)/P(\sigma_t > 0)$) vs. time (black dots). The solid blue line corresponds to the RHS of Eq. 1. We see that the numerical results bear excellent correspondence with analytical calculations.

Further, we note from Eq. 26 that for long times, the variation of the mean of the distributions with time is expected to be linear (since the exponential term effectively drops out). This observation is substantiated in Fig. 4, where we extract the values of the means of the distributions at $t = 2$ through 12 seconds from the Gaussian fits depicted in Fig. 2, and fit these to a linear model. We see that the values of the means fit reasonably well to this linear model, in accord with analytical calculations.

Quartic potential well

A similar analysis numerical has been carried out for the case of a uniformly accelerating quartic potential well (that moves in a viscous fluid), within which a Brownian particle is confined. For this, we set $n = 2$ in Eq. 14 to numerically compute
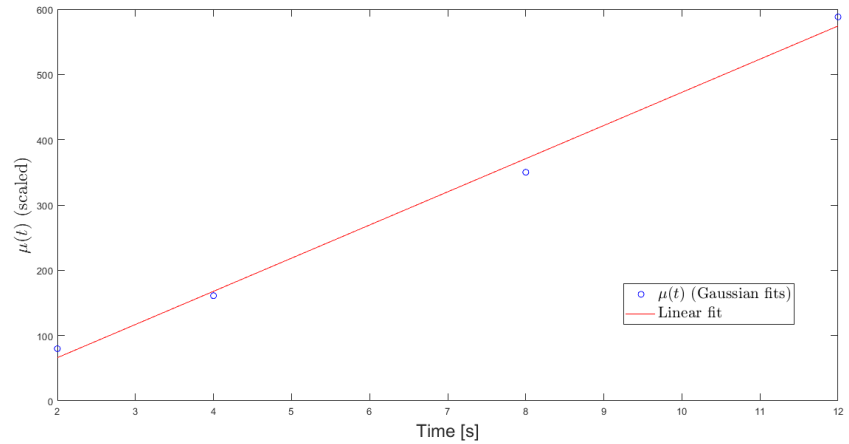
Fig 4. (Color outline) Linear fitting of the values of the means of the probability distributions extracted from the Gaussian fits in Fig. 2.
Plot for the variation of the means of the probability distributions (of σ_t) vs. time (blue hollow circles). The solid red line corresponds to the linear fit to the values of the means with 95% confidence bounds. Note that we extract the values of the distribution means (computed at $t = 2$ through 12 seconds) from the Gaussian fits depicted in Fig. 2.

and model the probability distribution of σ_t at different instances of time. Akin to the case of the harmonic trap, we consider the entropy-consumption and/or production along classical trajectories of different lengths (i.e., sampled over different time scales).
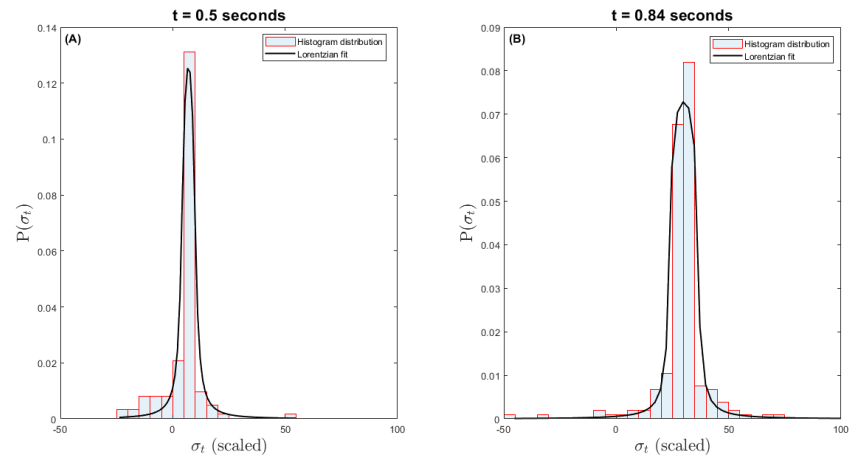
Fig 5. (Color outline) Lorentzian fits to the probability distributions of the stochastic work done by a Brownian particle confined within a uniformly accelerating quartic potential well at times closer to the initial transient.
A) Probability distribution of σ_t (stochastic work) computed at $t = 0.5$ seconds. **B**) Probability distribution of σ_t (stochastic work) computed at $t = 0.84$ seconds.

Dissimilarities between the harmonic trap and the quartic potential well cases become evident. In particular, we see that the probability distributions for $P(\sigma_t)$ in the case of the quartic confining potential assume a Lorentzian profile for different time instances. This is in contrast with what we observe and/or expect in the case of the harmonic trapping potential, where the distributions are Gaussian. At times closer to

the initial transient, we see that there exists a finite probability of observing entropy-consuming trajectories. This is evident from Fig. 5, where we see that the tails of the distributions extend towards negative values of σ_t. Also to be noted is the fact that given the apparent Lorentzian nature of the distribution profiles, the tails of the distributions decay more slowly as compared to the Gaussian profiles one expects for an $\sim x^2$ trapping potential. In any case, we see that the distributions are not stationary, but tend to evolve towards positive values of σ_t.
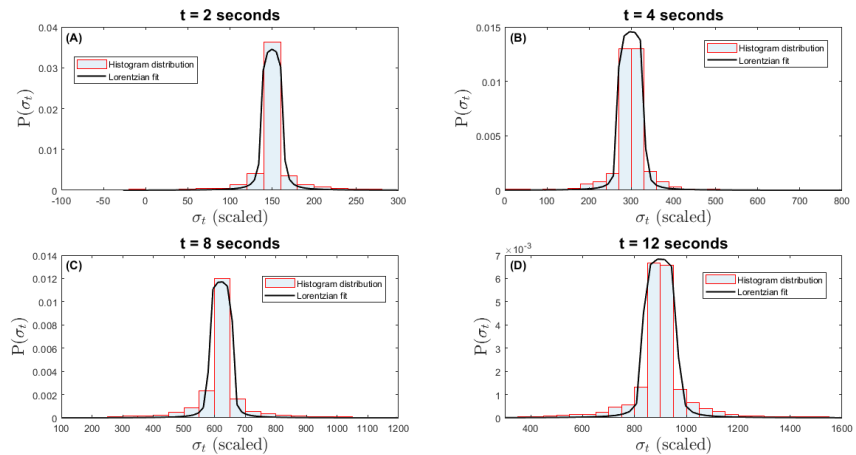
Fig 6. (Color outline) Lorentzian fits to the probability distributions of the stochastic work done by a Brownian particle confined within a uniformly accelerating quartic potential well at longer times.
A) Probability distribution of σ_t (stochastic work) computed at $t = 2$ seconds. **B**) Probability distribution of σ_t (stochastic work) computed at $t = 4$ seconds. **(C)** Probability distribution of σ_t (stochastic work) computed at $t = 8$ seconds. **(D)** Probability distribution of σ_t (stochastic work) computed at $t = 12$ seconds.

An important point to consider is the probability of observing entropy-consuming trajectories over certain time scales. To be noted from Fig. 6 is the fact that for times $\geq$ 2 seconds, the probability of observing entropy-consuming trajectories reduces to zero. On the other hand, we see that for times below 1 second (more specifically, 0.5 seconds and 0.84 seconds, as depicted in Fig. 5), there exists a finite probability of observing phase-space classical anti-trajectories (with the tail of the distributions extending towards negative values of σ_t). A further verification of this observation is presented in Fig. 7, where we note the rapid decrease in the probability of observing phase-space classical anti-trajectories. We see that the probability $P(\sigma_t < 0)$ is finite for times below 1 second, which beyond 1 second effectively vanishes. This is also in accord with Eq. 1, which predicts the exponential decrease of $P(\sigma_t < 0)$ with time, until a point after which no entropy-consuming trajectories are observed.
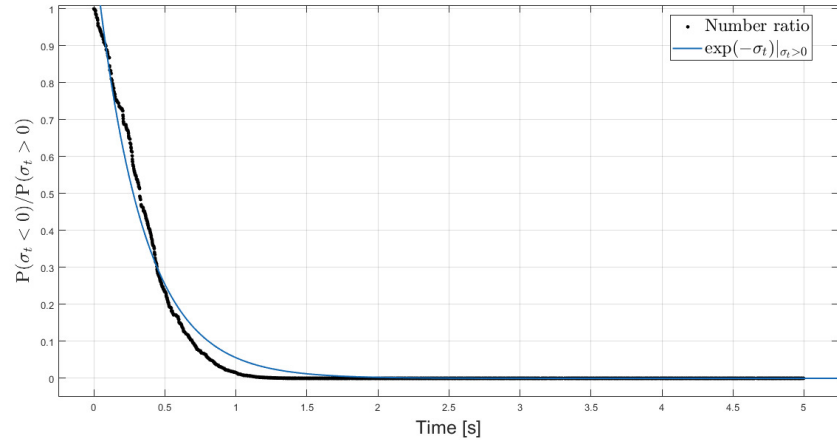
Fig 7. (Color outline) Plot for the number ratio of entropy-consuming to entropy-producing classical trajectories vs. time.
Plot for the number ratio of entropy-consuming to entropy-producing classical trajectories (i.e., $P(\sigma_t < 0)/P(\sigma_t > 0)$) vs. time (black dots). The solid blue line corresponds to the RHS of Eq. 1. We see that the numerical results bear reasonably good correspondence with analytical calculations.

Discussion

For the numerical analysis carried out in the previous section, it is important to emphasize that the system must evolve from an initial equilibrium steady-state. The analytical calculations as such do not incorporate phase-space compression factors. A detailed derivation of the stochastic work done along transient classical trajectories for a nearly similar model and/or scenario that considers thermostatting constraints and phase-space compression factors can be found in Ref. [41]. In Ref. [41], the authors consider a stationary trap (as opposed to the trap in motion analyzed in this paper) whose stiffness constant increases with time, starting from $t = 0$. One can infer from the analysis that if the trap contained no Brownian particle, no energy would be dissipated in translating it linearly [10]. Essentially, the numerical results suggest that heat and/or thermal fluctuations in the surroundings (which in our case, is the viscous fluid) were converted to useful work for up to a few seconds (about 0.5 seconds in the case of the moving harmonic trap and about a second in the case of the moving quartic potential well), beyond which the probability of this happening dwindled to zero. As to why the system must evolve from an initial equilibrium steady-state can be seen from Eq. 25: the derivation involves knowing the distribution of the initial particle positions. This implies that under the given conditions, it would not be possible to deduce analytically a closed-form expression for $P(\sigma_t)$ if the system were allowed to evolve from an initial non-equilibrium steady-state, since knowing $P(x_0)$ exactly in such a case would not be possible. Also to be noted is that the deviations in Figs. 3 and 7 seemingly arise because we approximate the transient fluctuation theorem with an approximate form of the dissipation function σ_t (in the steady-state). This thus corresponds to an approximation to the transient fluctuation theorem that holds true in the asymptotic (long-time) limit [10]. The integration over time, as seen in Eq. 14, starts from an initial equilibrium steady-state distribution, where the form of the dissipation function as deduced in Eq. 14 satisfies the transient fluctuation theorem in the long-time limit.

For the probability distribution of σ_t along transient classical trajectories in the case of the harmonic trapping potential, we see from Eq. 27 that the distribution tends to

move towards positive σ_t with the passage of time. Moreover, it can be seen that the spread of the distribution increases with time. This result is verified in Figs. 2 and 4. A possible physical interpretation of this is that it merely represents the dissipation production as the Brownian particle is dragged along with the trap (note that it is confined within the trap) with an acceleration a_{trap} [10]. We see that at sufficiently long times, the mean of the distribution of σ_t scales as $\propto t$ [see Eq. 26], which has been verified in Fig. 4 for the harmonic trap case. In the limit of sufficiently large t, we see that from Eq. 26, $\phi(t)$ assumes the form $\phi(t) = a_{\text{trap}}^2 \gamma^3/(k^2 k_B T)t - a_{\text{trap}}^2 \gamma^4/(k^3 k_B T)$. The first term contributing to the evolution of the mean at long times arises from the dissipation production discussed above, whereas the second term is a contribution arising from the initial translation of the trap in the viscous medium [10]. Furthermore, it is important to note that owing to the Gaussian nature of $P(\sigma_t)$ for the $\sim x^2$ confining potential, σ_t can assume both positive and negative values, as one can see for times very close to the initial transient. As such, it can be concluded that if the classical system happens to be fluctuating around equilibrium, there exists an equal probability for σ_t to assume positive and negative values, with the distribution centred at $\sigma_t = 0$. However, once the system enters a non-equilibrium steady-state (in our case, this corresponds to the translation of the trap at a uniform acceleration), the symmetry that $P(\sigma_t)$ exhibits in the equilibrium case vanishes, and the mean of the distribution evolves towards positive σ_t [42]. A detailed argument can be found in Ref. [42]. For the quartic confining potential, the numerical results suggest that the distributions for σ_t assume a Lorentzian profile at different instances of time. Given this, the tails of the distributions decay more slowly as compared to a typical Gaussian distribution. Figs. 3 and 7 confirm this, in that a slower decay for the number ratio of entropy-consuming to entropy-producing trajectories can be observed for the quartic confining potential case. It is, in any case, quite clear from Figs. 5 and 6 that the distributions evolve towards positive values of σ_t with the passage of time, an observation consistent with the fact that we are dealing with a classical system in a non-equilibrium steady-state.

In what follows, a select few of the applications of fluctuation theorems are summarized and discussed. Micro-sized and nano-sized machines that are primarily entropy-driven can be realized in principle for a myriad of medical and industrial applications [43], [44]. More recently, significant advances made in the area of stochastic thermodynamics have shown that in far-from-equilibrium classical systems, random fluctuations are naturally constrained by the rate of entropy production through certain thermodynamic uncertainty relations [45]– [48]. To this effect, the thermodynamics of quantum nanomachines and qubit engines have been studied extensively, the results of which serve as a positive reinforcement to the idea that power outputs for certain thermodynamic configurations can be enhanced within a particular regime of entropy production. In mechanobiology in particular, the fluctuation theorem can be applied to the real-time analysis of the thermodynamic properties of motor proteins in solution [49]– [51]. A comprehensive review of the study of far-from-equilibrium driven systems appeared in 2013 [52]. Studies pertaining to the analysis of nonequilibrium systems in the absence of detailed balance conditions have also appeared in recent years. Cengio *et al.* for instance, provide a comprehensive study of situations wherein detailed balance is broken in nonequilibrium systems and how this relates to the resulting violations of the fluctuation-dissipation theorem [53]. In essence, the authors exploit the fact that detailed balance is broken to establish and/or derive general constraints on nonequilibrium steady-states. Ouldridge in his 2017 paper highlights the importance of thermodynamical fluctuation theorems at the molecular level [54], especially with regards to the design and realization of nanoscale self-assembling systems. Studies linking stochastic thermodynamics with information theory have been undertaken over the recent years. Dinis *et al.* for instance, demonstrate that by reversibly confining a

Brownian particle in an optical trap, it is possible to extract the resulting increase in the free energy of the system as useful work [55]. Furthermore, they show that by repeatedly modulating the optical trap potential and by tracking the Brownian particle in real-time, it becomes possible to extract an optimal amount of work from the system, even when high degrees of inaccuracies in the measurements are introduced. Recently, Ito discussed a link between stochastic thermodynamics and information theory, in that he demonstrates that it is possible to interpret an information geometric inequality as a thermodynamic uncertainty relationship between speed and thermodynamic cost [56]. A central result of nonequilibrium statistical mechanics is the formulation of an exact closed-form expression for the entropy flow out of a classical system that undergoes dynamical evolution, starting from a given initial distribution over thermodynamic states. In computer science, this result plays an especially crucial role for analyzing how the total entropy flow out of a computing device depends on its global structure which in turn determines the initial distributions into all of the computing device's subsystems [57]. Wolpert in his 2018 paper illustrates at length the application of this result and other related results to investigate the thermodynamics of computation and information retrieval [57]. A recent important work pertaining to the determination of thermodynamic uncertainty relations surfaced in 2019 [58]. Ref. [58] in particular presents a detailed derivation of a thermodynamic uncertainty relation from the fluctuation theorem which is shown to be valid for arbitrary dynamics, be it deterministic or stochastic. Most importantly, the authors demonstrate that the thermodynamic uncertainty relation holds true when applied to an asymmetric observable of a system obeying overdamped Langevin dynamics. In addition, the authors show that the thermodynamic uncertainty relation applies to systems governed and/or controlled by external time-symmetric protocols, in which the lower bound on uncertainty is determined through the work exerted on such systems [58].

Conclusion

In this paper, we demonstrate the applicability of the transient fluctuation theorem to a classical system consisting of a Brownian particle confined within a uniformly accelerating power-law trap. We consider two such special cases, one corresponding to a harmonic trap and the other corresponding to a quartic potential well. For the harmonic trap case, we derive an approximate analytical expression for the stochastic work done by the Brownian particle over transient classical trajectories of different lengths (i.e., over different time scales) and thereafter, a closed-form expression for the probability distribution for the stochastic work as a function of time. We see that the probability distribution for σ_t (i.e., the stochastic work) for a Brownian particle confined within a uniformly accelerating harmonic trap assumes a Gaussian profile for all times $t > 0$. On the other hand, it is observed that the distribution for σ_t for a quartic confining potential is Lorentzian in nature for different time instances, in direct contrast with the numerical results obtained for the harmonic trap case. We see that the analytical results (the key results being Eq. 14 and Eq. 27) are in good agreement with numerical results, thus demonstrating that the form of the dissipation function deduced in Eq. 14 satisfies the transient fluctuation theorem in the asymptotic (long-time) limit. In conclusion, it can also be said that given a finite probability of observing phase-space classical anti-trajectories over certain time scales, the study of the role of non-equilibrium steady-states in the manifestation of time symmetry-breaking in classical systems could prove to be an interesting and fruitful venture in the near future [42].

Supporting information

Data Availability Statement: DOI for simulation codes deposited at Zenodo: `https://doi.org/10.5281/zenodo.5573326` [59].

Acknowledgments

The author (Y.L.) would like to express his gratitude to his former mentor, D.R.M. Williams for his generous support. This research did not receive any specific grant from funding agencies in the public, commercial or not-for-profit sectors.

Conflict of interest: The author declares no competing interests.

References

1. Seifert U. Stochastic thermodynamics, fluctuation theorems and molecular machines. Rep. Prog. Phys. 2012 Nov; 75, 126001.

2. Sharp K., Matschinsky F. Translation of Ludwig Boltzmann's Paper "On the Relationship between the Second Fundamental Theorem of the Mechanical Theory of Heat and Probability Calculations Regarding the Conditions for Thermal Equilibriu" Sitzungberichte der Kaiserlichen Akademie der Wissenschaften. Mathematisch-Naturwissen Classe. Abt. II, LXXVI 1877, pp 373-435 (Wien. Ber. 1877, 76:373-435). Reprinted in Wiss. Abhandlungen, Vol. II, reprint 42, p. 164-223, Barth, Leipzig, 1909 Entropy 2015 April; 17(4):e17041971.

3. Wang G.M., Sevick E.M., Mittag E., Searles D.J., Evans D.J. Experimental Demonstration of Violations of the Second Law of Thermodynamics for Small Systems and Short Time Scales. Phys. Rev. Lett. 2002 July; 89, 050601.

4. Loschmidt J., Sitzungsber J. der kais. Akad. d. W. Math. Naturw. 1876; II 73, 128.

5. Busiello D.M., Gupta D., Maritan A. Coarse-grained entropy production with multiple reservoirs: Unraveling the role of time scales and detailed balance in biology-inspired systems. Phys. Rev. Research 2020 Nov; 2, 043257.

6. Busiello D.M., Gupta D., Maritan A. Entropy production in systems with unidirectional transitions. Phys. Rev. Research 2020 April; 2, 023011.

7. Speck T., Blickle V., Bechinger C., Seifert U. Distribution of entropy production for a colloidal particle in a nonequilibrium steady state. EPL July 2007; 79, 30002.

8. Seifert U. Entropy Production along a Stochastic Trajectory and an Integral Fluctuation Theorem. Phys. Rev. Lett. July 2005; 95, 040602.

9. Carberry D.M., Reid J.C., Wang G.M., Sevick E.M., Searles D.J., Evans D.J. Fluctuations and Irreversibility: An Experimental Demonstration of a Second-Law-Like Theorem Using a Colloidal Particle Held in an Optical Trap. Phys. Rev. Lett. April 2004; 92, 140601.

10. Wang G.M., Reid J.C., Carberry D.M., Williams D.R.M., Sevick E.M., Evans D.J. Experimental study of the fluctuation theorem in a nonequilibrium steady state. Phys. Rev. E April 2005; 71, 046142.

11. Carberry D.M., Baker M.A.B., Wang G.M., Sevick E.M., Evans D.J. An optical trap experiment to demonstrate fluctuation theorems in viscoelastic media. J. Opt. A: Pure Appl. Opt. July 2007; 9, S204.

12. Evans D.J., Cohen E.G.D., Morriss G.P. Probability of second law violations in shearing steady states. Phys. Rev. Lett. Oct 1993; 71, 2401.

13. Evans D.J., Searles D.J. Equilibrium microstates which generate second law violating steady states. Phys. Rev. E Aug 1994; 50, 1645.

14. Crooks G.E. Entropy production fluctuation theorem and the nonequilibrium work relation for free energy differences. Phys. Rev. E Sept 1999; 60, 2721.

15. Crooks G.E. Path-ensemble averages in systems driven far from equilibrium. Phys. Rev. E March 2000; 61, 2361.

16. Jarzynski C. Nonequilibrium Equality for Free Energy Differences. Phys. Rev. Lett. April 1997; 78, 2690.

17. Gallavotti G., Cohen E.G.D. Dynamical Ensembles in Nonequilibrium Statistical Mechanics. Phys. Rev. Lett. April 1995; 74, 2694.

18. Lepri S., Rondoni L., Benettin G. The Gallavotti–Cohen Fluctuation Theorem for a Nonchaotic Model. Journal of Statistical Physics May 2000; 99, 857-872.

19. Ruelle D. Smooth Dynamics and New Theoretical Ideas in Nonequilibrium Statistical Mechanics. Journal of Statistical Physics April 1999; 95, 393-468.

20. Maes C., Redig F. Positivity of Entropy Production. Journal of Statistical Physics Oct 2000; 101, 3-15.

21. Searles D.J., Evans D.J. Ensemble dependence of the transient fluctuation theorem. J. Chem. Phys. Aug 2000; 113, 3503.

22. Ayton G., Evans D.J., Searles D.J. A local fluctuation theorem. J. Chem. Phys. July 2001; 115, 2033.

23. Evans D.J., Searles D.J., Mittag E. Fluctuation theorem for Hamiltonian Systems: Le Chatelier's principle. Phys. Rev. E April 2001; 63, 051105.

24. Evans D.J., Searles D.J. The Fluctuation Theorem. Adv. Phys. Nov 2002; 51:7, 1529-1585.

25. Zon van R., Cohen E.G.D. Stationary and transient work-fluctuation theorems for a dragged Brownian particle. Phys. Rev. E April 2003; 67, 046102.

26. Carberry D.M., Reid J.C., Wang G.M., Sevick E.M., Searles D.J., Evans D.J. Fluctuations and Irreversibility: An Experimental Demonstration of a Second-Law-Like Theorem Using a Colloidal Particle Held in an Optical Trap. Phys. Rev. Lett. April 2004; 92, 140601.

27. Blickle V., Speck T., Helden L., Seifert U., Bechinger C. Thermodynamics of a Colloidal Particle in a Time-Dependent Nonharmonic Potential. Phys. Rev. Lett. Feb 2006; 96, 070603.

28. Narayan O., Dhar A. Reexamination of experimental tests of the fluctuation theorem. J. Phys. A: Math. Gen. Oct 2003; 37, 63-76.

29. Liphardt J., Dumont S., Smith S.B., Tinoco I., Bustamante C. Equilibrium Information from Nonequilibrium Measurements in an Experimental Test of Jarzynski's Equality. Science June 2002; vol. 296, no. 5574, pp. 1832-1835.

30. Wang G.M., Carberry D.M., Reid J.C., Sevick E.M., Evans D.J. Demonstration of the steady-state fluctuation theorem from a single trajectory. J. Phys.: Condens. Matter Nov 2005; 17, S3239.

31. Pal A., Sabhapandit S. Work fluctuations for a Brownian particle in a harmonic trap with fluctuating locations. Phys. Rev. E Feb 2013; 87, 022138.

32. Gieseler J., Quidant R., Dellago C., Novotny L. Dynamic relaxation of a levitated nanoparticle from a non-equilibrium steady state. Nature Nanotechnology March 2014; 9, 358-364.

33. Gieseler J., Millen J. Levitated Nanoparticles for Microscopic Thermodynamics—A Review. Entropy April 2018; 20(5), 326.

34. Narinder N., Paul S., Bechinger C. Work fluctuation relation of an active Brownian particle in a viscoelastic fluid. Phys. Rev. E Sept 2021; 104, 034605.

35. Bérut A., Imparato A., Petrosyan A., Ciliberto S. Stationary and Transient Fluctuation Theorems for Effective Heat Fluxes between Hydrodynamically Coupled Particles in Optical Traps. Phys. Rev. Lett. Feb 2016; 116, 068301.

36. Dabelow L., Bo S., Eichhorn R. Irreversibility in Active Matter Systems: Fluctuation Theorem and Mutual Information. Phys. Rev. X April 2019; 9, 021009.

37. Dabelow L., Eichhorn R. Irreversibility in Active Matter: General Framework for Active Ornstein-Uhlenbeck Particles. Front. Phys. Jan 2021; 8:582992.

38. Martínez A.I., Roldań E., Dinis L., Rica R.A. Colloidal heat engines: a review. Soft Matter July 2016; 13, 22-36.

39. Gomez-Solano J.R. Work Extraction and Performance of Colloidal Heat Engines in Viscoelastic Baths. Front. Phys. March 2021; 9:643333.

40. Holubec V., Steffenoni S., Falasco G., Kroy K. Active Brownian heat engines. Phys. Rev. Research Nov 2020; 2, 043262.

41. Reid J.C., Carberry D.M., Wang G.M., Sevick E.M., Evans D.J., Searles D.J. Reversibility in nonequilibrium trajectories of an optically trapped particle. Phys. Rev. E July 2004; 70, 016111.

42. Nicolis G., Decker De Y. Stochastic Thermodynamics of Brownian Motion. Entropy Aug 2017; 19(9), 434.

43. Ma F., Wei S., Zhang C. Construction of a Robust Entropy-Driven DNA Nanomachine for Single-Molecule Detection of Rare Cancer Cells. Anal. Chem. June 2019; 91, 12, 7505-7509.

44. Rocha B.C., Paul S., Vashisth H. Role of Entropy in Colloidal Self-Assembly. Entropy Aug 2020; 22(8), 877.

45. Rignon-Bert A., Guarnieri G., Goold J., Mitchison M.T. Thermodynamics of precision in quantum nanomachines. Phys. Rev. E Jan 2021; 103, 012133.

46. Horowitz J.M., Gingrich T.R. Thermodynamic uncertainty relations constrain non-equilibrium fluctuations. Nature Physics March 2020; 16, 15-20.

47. Falasco G., Esposito M., Delvenne J. Unifying thermodynamic uncertainty relations. New J. Phys. May 2020; 22, 053046.

48. Kalaee A.A.S., Wacker A., Potts P.P. Violating the thermodynamic uncertainty relation in the three-level maser. Phys. Rev. E July 2021; 104, L012103.

49. Hayashi K., Tsuchizawa Y., Iwaki M., Okada Y. Application of the fluctuation theorem for noninvasive force measurement in living neuronal axons. Molecular Biology of the Cell Dec 2018; vol. 29, no. 25.

50. Hayashi K. Application of the fluctuation theorem to motor proteins: from F1-ATPase to axonal cargo transport by kinesin and dynein. Biophysical Reviews July 2018; 10, 1311-1321.

51. Damien R., Nguyen T., Gallet F., Wilhelm C. In Vivo Determination of Fluctuating Forces during Endosome Trafficking Using a Combination of Active and Passive Microrheology. PLoS ONE April 2010; 5(4): e10046.

52. Ciliberto S., Gomez-Solano R., Petrosyan A. Fluctuations, Linear Response, and Currents in Out-of-Equilibrium Systems. Annu. Rev. Condens. Matter Phys. April 2013; 4, 235-261.

53. Cengio S.D., Levis D., Pagonabarraga I. Fluctuation–dissipation relations in the absence of detailed balance: formalism and applications to active matter. J. Stat. Mech. April 2021; 043201.

54. Ouldridge T.E. The importance of thermodynamics for molecular systems, and the importance of molecular systems for thermodynamics. Natural Computing Nov 2017; 17, 3-29.

55. Dinis L., Parrondo J.M.R. Extracting Work Optimally with Imprecise Measurements. Entropy Dec 2020; 23(1), 8.

56. Ito S. Stochastic Thermodynamic Interpretation of Information Geometry. Phys. Rev. Lett. July 2018; 121, 030605.

57. Wolpert D.H. Overview of Information Theory, Computer Science Theory, and Stochastic Thermodynamics for Thermodynamics of Computation. Available at arXiv. `https://arxiv.org/abs/1901.00386v4`. Dec 2018.

58. Hasegawa Y., Van Vu T. Fluctuation Theorem Uncertainty Relation. Phys. Rev. Lett. Sept 2019; 123, 110602.

59. Lokare Y. Simulation codes: IFT_colloidal systems. Zenodo 2021; `https://doi.org/10.5281/zenodo.5573326`.